



Research article

Integrated single-cell and bulk RNA-sequencing data reveal molecular subtypes based on lactylation-related genes and prognosis and therapeutic response in glioma

Xiangdong Lu^{a,b,c}, Zijian Zhou^{d,e}, Peng Qiu^{f,g,h,**}, Tao Xin^{b,d,e,*}

^a Jiangxi Medical College, Nanchang University, Nanchang, 330031, Jiangxi, China

^b Department of Neurosurgery, Jiangxi Provincial People's Hospital, The First Affiliated Hospital of Nanchang Medical College, Nanchang, 330006, Jiangxi, China

^c Department of Neurosurgery, People's Hospital Affiliated to Shandong First Medical University, Jinan, 271100, Shandong, China

^d Department of Neurosurgery, The First Affiliated Hospital of Shandong First Medical University & Shandong Provincial Qianfoshan Hospital, Jinan, 250014, China

^e Medical Science and Technology Innovation Center, Shandong First Medical University and Shandong Academy of Medical Sciences, Jinan, 250117, China

^f Shandong University of Traditional Chinese Medicine, Jinan, 250355, China

^g Shandong Luoxin Pharmaceutical Group Stock Co., Ltd. China

^h Shandong Provincial Hospital Affiliated to Shandong First Medical University, China

ARTICLE INFO

Keywords:

scRNA-seq

Glioma

Prognostic signature

Lactylation

Immunotherapy response

ABSTRACT

Objectives: Glioma, the most common and aggressive form of brain cancer, possesses a complex biology, which makes elucidating its underlying mechanisms and developing effective treatment strategies challenging. Lactylation is a recently discovered post-translational modification and has emerged as a novel research target to understand its role in various biological processes and diseases. Herein, we explored the role of lactylation in gliomas.

Methods: Single-cell RNA-sequencing (scRNA-seq) data were downloaded from the Tumour Immune Single-Cell Hub database. The R package 'Seurat' was used for processing the scRNA-seq data. Lactylation-related genes were identified from published literature and the Molecular Signatures Database. An unsupervised clustering method was used to identify glioma subtypes based on identified lactylation-related genes. Differences among the various clusters were examined, including clinical features, differentially expressed genes (DEGs), enriched pathways and immune cell infiltrates. A lactylation score was generated to predict the overall survival (OS) of patients with glioma using DEGs between the two clusters.

Results: The lactylation-related genes were obtained from the scRNA-seq data, identifying two molecular subtypes, and a prognostic signature was established to stratify patients with glioma into high- and low-score groups. Analysis of the tumour immune microenvironment revealed that patients in the high-score group exhibited increased immune cell infiltration, chemokine expression and immune checkpoint expression but exhibited worse OS and better response to immunotherapy.

* Corresponding author. Department of Neurosurgery, The First Affiliated Hospital of Shandong First Medical University, No. 16766, Jingshi Road, Lixia District, Jinan, 250014, Shandong, China.

** Corresponding author. Department of Neurosurgery. Shandong University of Traditional Chinese Medicine, No. 16369, Jingshi Road, Lixia District, Jinan, 250355, Shandong, China.

E-mail addresses: qpk1007@163.com (P. Qiu), xintao@sdfmu.edu.cn (T. Xin).

<https://doi.org/10.1016/j.heliyon.2024.e30726>

Received 24 September 2023; Received in revised form 2 May 2024; Accepted 2 May 2024

Available online 6 May 2024

2405-8440/© 2024 Published by Elsevier Ltd.

This is an open access article under the CC BY-NC-ND license

(<http://creativecommons.org/licenses/by-nc-nd/4.0/>).

Conclusions: Altogether, we established a novel signature based on lactylation-related clusters for robust survival prediction and immunotherapeutic response in gliomas.

Abbreviations

scRNA-seq	Single-cell RNA-sequencing
DEGs	differentially expressed genes
OS	overall survival
TCGA	The Cancer Genome Atlas
GBMLGG	glioblastoma and low-grade glioma
CGGA	Chinese Glioma Genome Atlas
MsigDB	Molecular Signatures Database
GSVA	Gene set variation analysis
KEGG	Kyoto Encyclopedia of Genes and Genomes
GO	Gene Ontology
PCA	principal component analysis
IC50	50 % maximum inhibitory concentration
DCs	dendritic cells
CD	cluster of differentiation
ECM	extracellular matrix
AGE	advanced glycation end-product
CNVs	copy number variations
SNV	single nucleotide variant
ICI	immune checkpoint inhibitor
BP	biological progress
CC	cellular component
MF	molecular function
CAN	copy-number alteration

1. Introduction

Gliomas are the most prevalent primary brain tumour, constituting approximately 80 % of all malignant brain tumours [1]. Gliomas are a considerable public health concern because of their high morbidity and mortality rates, which place a substantial burden on healthcare systems worldwide. Primary brain tumours such as gliomas arise from glial cells and exhibit considerable heterogeneity, encompassing various subtypes with distinct genetic profiles and clinical behaviours. The complexity of gliomas poses challenges for accurate diagnosis, treatment planning and therapeutic outcomes. Despite advances in neuro-oncology, present treatment strategies have limitations in effectively targeting the diverse molecular characteristics of different glioma subtypes. This intricacy necessitates the development of innovative approaches to address the multifaceted nature of glioma management and improve patient outcomes [2].

Lactylation, a novel post-translational modification, has garnered attention in cancer research [3,4]. It involves the addition of lactate molecules to specific proteins, which leads to structural and functional alterations in the protein. It is an important modification in various cellular processes, including metabolism, signalling pathways and epigenetic regulation [5]. Recent studies have reported that lactylation is involved in normal cell physiology, tumourigenesis and tumour progression [6]. Aberrant lactylation occurs in various types of tumours, including breast [7], colorectal [8] and liver [9] cancers. Limited studies have been conducted on lactylation in gliomas. A study showed that histone lactylation-derived LINC01127 promotes the self-renewal of glioma stem cells via the *cis*-regulation of mitogen-activated protein kinase 4 to activate the Jun N-terminal kinase pathway [10]. Another study reported that the inhibition of ectonucleotidases and C-C motif chemokine receptor 8 lactylation can boost the effectiveness of the chimeric antigen receptor T cell therapy against glioma [11]. Studies have increasingly focused on elucidating the functional implications of lactylation and its underlying mechanisms in cancer. Herein, we aimed to identify the subtypes of glioma using unsupervised clustering by conducting an in-depth analysis of lactylation-related genes, indicating the necessity for further exploration of lactylation-related mechanisms. Furthermore, we have compared the two clusters for their clinical characteristics, differentially expressed genes (DEGs), enriched pathways and immune cell infiltration. Additionally, we have developed a lactylation score to accurately predict the overall survival (OS) of patients with gliomas. The correlation between lactylation score and the immune microenvironment of tumours, along with the potential efficacy of immunotherapy was examined in this study.

2. Materials and methods

2.1. Data source and processing

The single-cell RNA sequencing (scRNA-seq) dataset GSE162631, containing four adult primary tumour samples and four paired surrounding peripheral tissues, was obtained from the Tumour Immune Single-Cell Hub database (tisch.comp-genomics.org/home/). Herein, we only included the four adult primary tumour samples. The messenger RNA (mRNA) expression profiles and clinical data for The Cancer Genome Atlas (TCGA)- glioblastoma and low-grade glioma (GBMLGG) (670 tumour tissues) were downloaded from the UCSC-Xena database (<https://xenabrowser.net/datapages/>), whereas Chinese Glioma Genome Atlas (CGGA) mRNAseq_693 (693 tumour tissues) and CGGA mRNAseq_325 (325 tumour tissues) data were downloaded from the CGGA database (<http://www.cgga.org.cn/>). The R packages, 'limma' and 'sva,' were utilised to remove batch effects. Lactylation-related genes have not been fully identified. Therefore, we selected lactate metabolism-related genes and combined them with the findings of published studies on lactylation to identify lactylation-related genes. The gene sets for lactylation genes were acquired from the Molecular Signatures Database (MsigDB) (GOBP_LACTATE_METABOLIC_PROCESS: http://www.gsea/msigdb.org/gsea/msigdb/human/geneset/GOBP_LACTATE_METABOLIC_PROCESS and GOBP_LACTATE_TRANSMEMBRANE_TRANSPORT: http://www.gseamsigdb.org/gsea/msigdb/human/geneset/GOBP_LACTATE_TRANSMEMBRANE_TRANSPORT) and the published literature [12]. In total, 34 lactylation-related genes were identified.

2.2. scRNA-seq analysis

The scRNA-seq data were screened and analysed using the R package 'Seurat.' First, the quality control analysis of scRNA-seq data was performed using the following criteria: 1) excluding genes overlapping in less than five cells; 2) eliminating cells with expression of <300 and >5000 genes; 3) removing cells with >5 % mitochondrial gene expression; 4) retaining cells with ribosomal gene expression of >3 % and 5) including cells with haemoglobin gene expression of <0.1 %. Next, the 'harmony' R package was used to reduce the batch effect between samples and the scRNA-seq data was normalised using 'ScaleData' to subsequently perform principal component analysis (PCA). The 'UMAP' function was used to reduce dimensionality, and 'FindAllMarkers' was used to identify DEGs in different clusters. Finally, cells were clustered at a resolution of 0.8, and cell annotation was performed using the 'singleR' package combined with manual adjustment. The R package 'GSVA' was used to calculate scores of lactylation in each cell based on lactylation-related genes. Additionally, cell communication analysis was performed using the R package 'CellChat.'

2.3. Consensus clustering analysis

A consensus clustering analysis was performed on the samples of the testing set with the R package 'ConsensusClusterPlus' to identify glioma subtypes based on lactylation-related genes. Next, the optimum cluster numbers between $k = 2$ and $k = 10$ were identified, following which the procedure was repeated 1000 times to ensure the robustness and reproducibility of the findings. A cluster map was created using the pheatmap function in the R software.

2.4. Gene set variation analysis (GSVA) and immune cell infiltration analysis

The differences in pathways among the various subtypes were evaluated by separately downloading the HALLMARK, Kyoto Encyclopedia of Genes and Genomes (KEGG) and Reactome pathways from the MSigDB (<http://www.gsea-msigdb.org/gsea/index.jsp>) and estimating the scores using the R package, 'GSVA.' The immune, stromal and ESTIMATE scores of patients with glioma were calculated using the R package 'ESTIMATE,' and the fraction of immune cell infiltration was calculated using the 'ssGSEA' function of the R package 'GSVA' to compare the differences in immune cell infiltration among subtypes.

2.5. Construction of the prognostic signature

First, differential analyses were performed for each of the two subtypes, and 160 genes with a $\log_2(\text{fold change})$ of >2 and p-value of <0.05 were considered DEGs. These DEGs were pooled to obtain a gene set, and their functional enrichment was assessed by Gene Ontology (GO)/KEGG analyses using the R package 'clusterProfiler.' Next, all 160 DEGs were subjected to univariate Cox regression analysis, and the top 20 genes with the lowest prognosis-associated p-values were identified. Finally, the signature scores were calculated using PCA. Using principal components (PCs) 1 and 2, we obtained a lactylation score [13]. The score for each patient was obtained using the following formula:

$$\text{Score} = \sum (\text{PC1}_i) + \sum (\text{PC2}_i)$$

2.6. Relationship between the prognostic signature and immunotherapeutic response

Correlation analysis was performed to establish the association among the risk score, immune cell infiltration and 50 hallmark pathways to clarify the relationship between the risk score and the tumour immune microenvironment. A correlation was considered significant when the p-value was <0.05. Additionally, the expression of various chemokines and immune checkpoints were compared

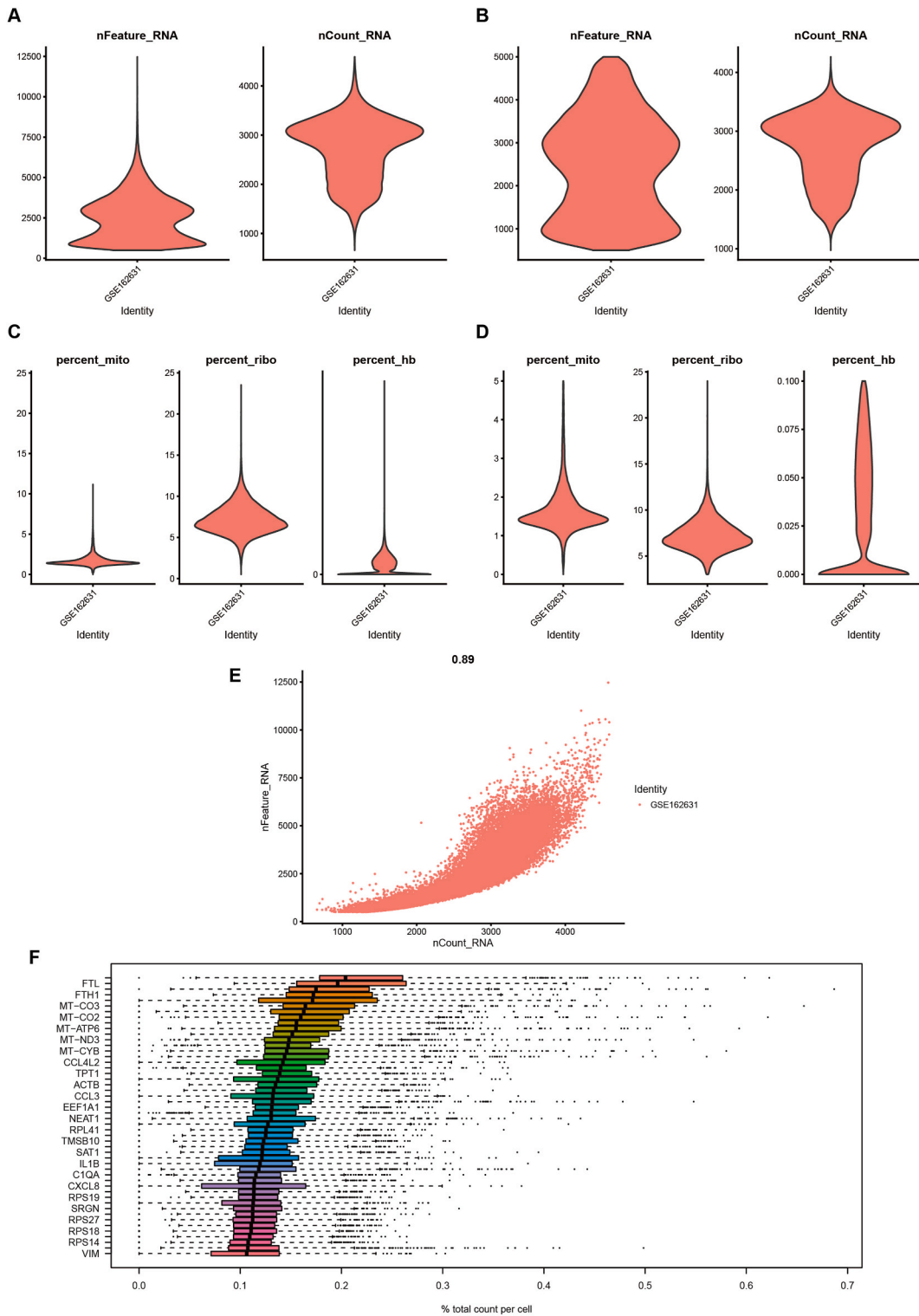


Fig. 1. Quality control of the single-cell RNA sequencing data

A-B. The nFeature_RNA and nCount_RNA value before (A) and after (B) the quality control. C-D. The percentage of mitochondrial/ribosomal/haemoglobin content before (C) and after (D) the quality control. E. Correlation between the nFeature_RNA and nCount_RNA. F. The top 25 genes with the highest percentage of cellular expression.

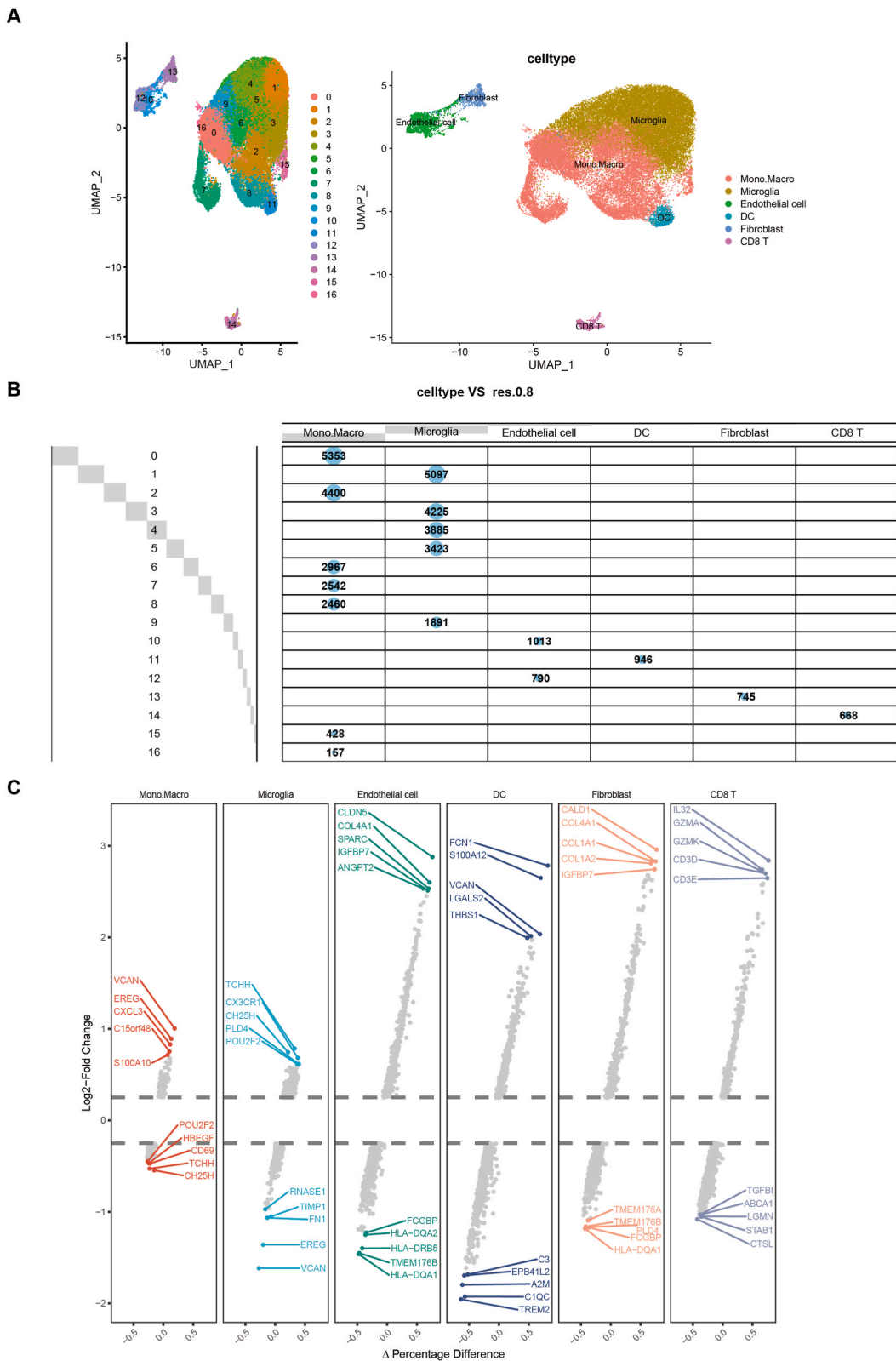


Fig. 2. Cell type identification

A. The clusters and cell types of GSE162631. B. The number of cells in each cluster and cell type. C. The top five up-regulated and down-regulated differentially expressed genes of each cell type.

between the high- and low-score groups to determine the association between the risk score and immunotherapy response. Moreover, the effectiveness of the risk scores in predicting immunotherapy was confirmed in the following three cohorts: GSE78220, Riaz2017, and NCT02684006.

2.7. Drug sensitivity analysis

Focusing on targeted therapies, the 50 % maximum inhibitory concentration (IC50) of each sample to multiple anti-cancer drugs was estimated using the R package ‘pRRophetic.’ The differences in IC50 values between the high- and low-score groups were compared, with a higher IC50 indicating low treatment sensitivity, to explore the direction of treatment for immunotherapy-insensitive cases.

2.8. Statistical analyses

Data are presented as means ± standard error. Differences between groups were analysed using the student’s t-test. Statistical analyses were performed using the R version 4.2.2. Statistical significance was set at $p < 0.05$ (two-tailed).

3. Results

3.1. Lactylation-related genes in scRNA-seq data

The scRNA-seq data were screened. Fig. 1 shows the range of detected gene numbers before (Fig. 1A) and after (Fig. 1B) the quality control, and the percentage of mitochondrial/ribosomal/haemoglobin content in each sample before (Fig. 1C) and after (Fig. 1D) the quality control. The nFeature_RNA value positively correlated with the nCount_RNA value (Fig. 1E). The top 25 genes with the highest expression are shown in Fig. 1F.

After dimensionality reduction, 17 clusters were identified and annotated into six core cell types, namely mono, macro, microglia, endothelial cells, dendritic cells (DCs), fibroblasts, and cluster of differentiation (CD)8 T cells (Fig. 2A). Fig. 2B shows the number of cells in each cluster and the cell type. DEG analysis of each cell type revealed the top five upregulated and downregulated genes in cell types (Fig. 2C).

Next, we calculated the lactylation score and 50 hallmark pathways using the scRNA-seq data. Fig. 3A shows the scores of 50 hallmark pathways in each cell type, presenting the characteristics of each cell type. For example, the EPITHELIAL MESENCHYMAL TRANSITION and ANGIOGENESIS pathways were highly enriched in endothelial and fibroblast cells. We further explored the correlation between lactylation and 50 hallmark pathways in each cell type (Fig. 3B). The results showed that the lactylation process was

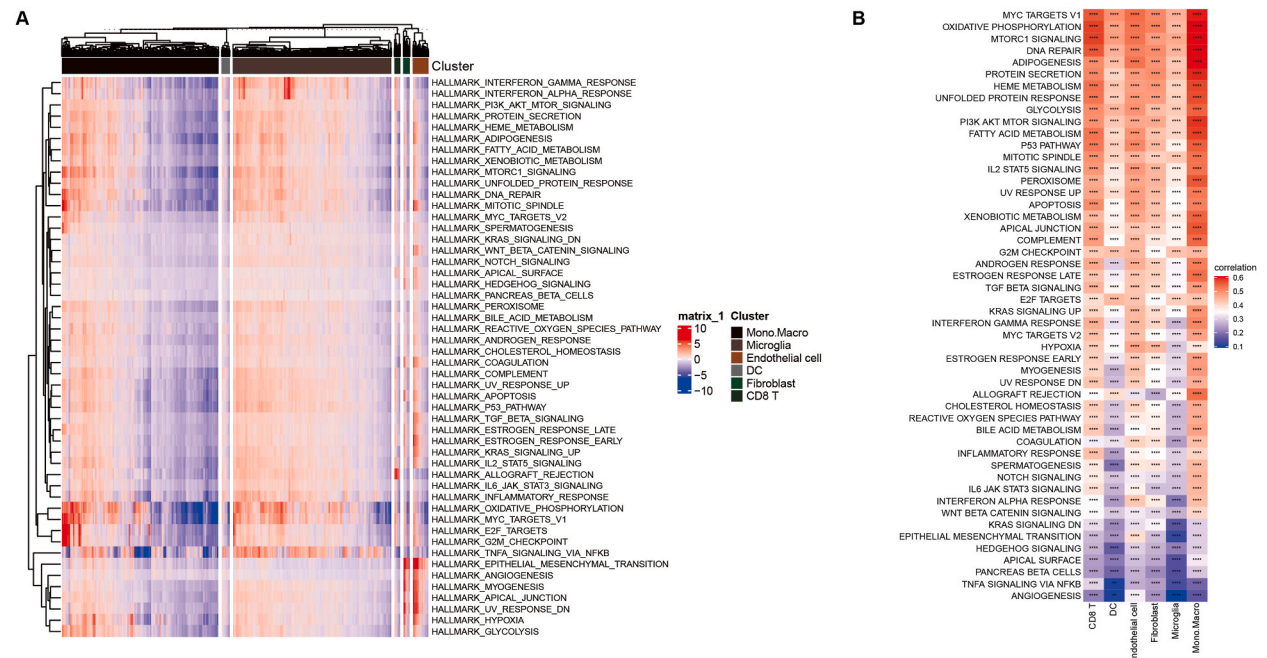


Fig. 3. Pathway analysis
 A. Heatmap showing the scores of 50 hallmark pathways in each cell type. B. The correlation of lactylation score with 50 hallmark pathways in each cell type.

closely associated with ADIPOGENESIS, DNA REPAIR, MTORC1 SIGNALING and OXIDATIVE PHOSPHORYLATION pathways in all cell types. Fig. 4A shows the expression of the lactylation-related genes in the indicated cell types. For example, lactate dehydrogenase A was generally expressed in all six cell types. Fig. 4B shows that microglial cells had the highest lactylation score, whereas fibroblast cells had the lowest. All cells were categorised into high and low lactylation score groups based on the median lactylation score (Fig. 4C). The high lactylation score group contained a higher percentage of microglial cells compared with the percentage in the low lactylation score group (Fig. 4D). Fig. 4E shows that the high lactylation score group was predominantly enriched in oncogenic malignant pathways.

3.2. Identification of lactylation gene-related subtypes

The expression profiles of tumour tissues from TCGA and CGGA were combined, and the prognostic significance of lactylation-related genes was evaluated using univariate Cox regression and Kaplan–Meier analysis. The results of univariate Cox regression and correlation analysis of lactylation genes are shown in Fig. 5A. Fig. 5B illustrates the association between lactylation-related genes and patient prognosis. Gliomas were then divided into two subtypes, namely clusters A and B, based on the expression patterns of lactylation-related genes (Fig. 6A). Patients in cluster B exhibited poorer survival rates than those in cluster A (Fig. 6B). The distribution of clinical features and lactylation-related gene expression in each cluster is presented (Fig. 6C and D).

The differences between the two clusters in various pathways were investigated using GSVA. The findings showed that most of the HALLMARK, KEGG, and Reactome pathways exhibited higher scores in cluster B, especially some immune-related pathways (Fig. 7). For example, IL6_JAK_STAT3_SIGNALING, INFLAMMATORY_RESPONSE and L2_STAT5_SIGNALING in Hallmark; LEUKOCYTE_TRANSENDOTHELIAL_MIGRATION and CYTOKINE_CYTOKINE_RECEPTOR_INTERACTION in KEGG and INTERFERON_SIGNALING and INTERLEUKIN_7_SIGNALING in Reactome pathway. These findings suggest that the largest difference between the two subtypes was in carcinogenesis- and tumour immune microenvironment-associated pathways.

We evaluated the presence of immune infiltrates in glioma samples and observed notable differentiation between clusters A and B based on the PCA plot (Fig. 8A). The stromal, immune, and ESTIMATE scores were higher in cluster B (Fig. 8B), and cluster B

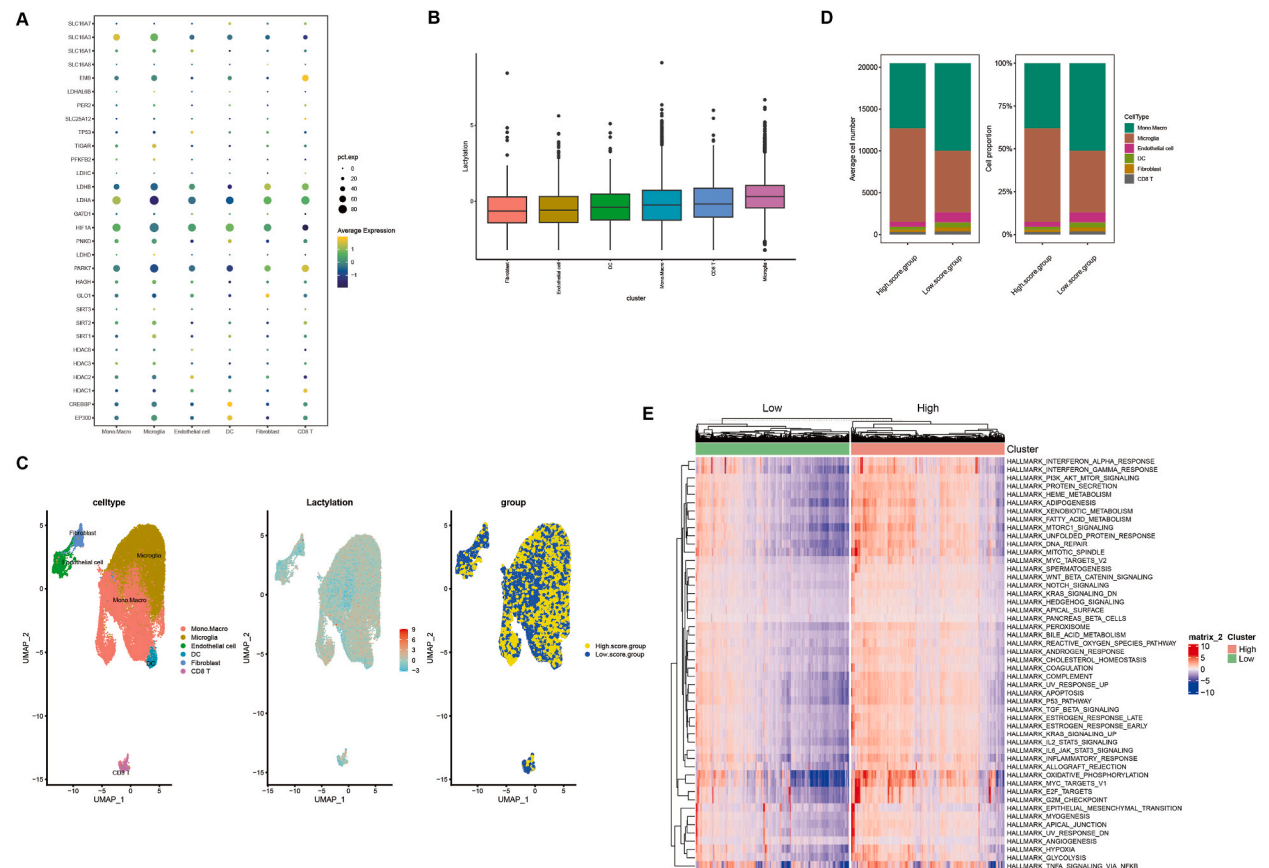
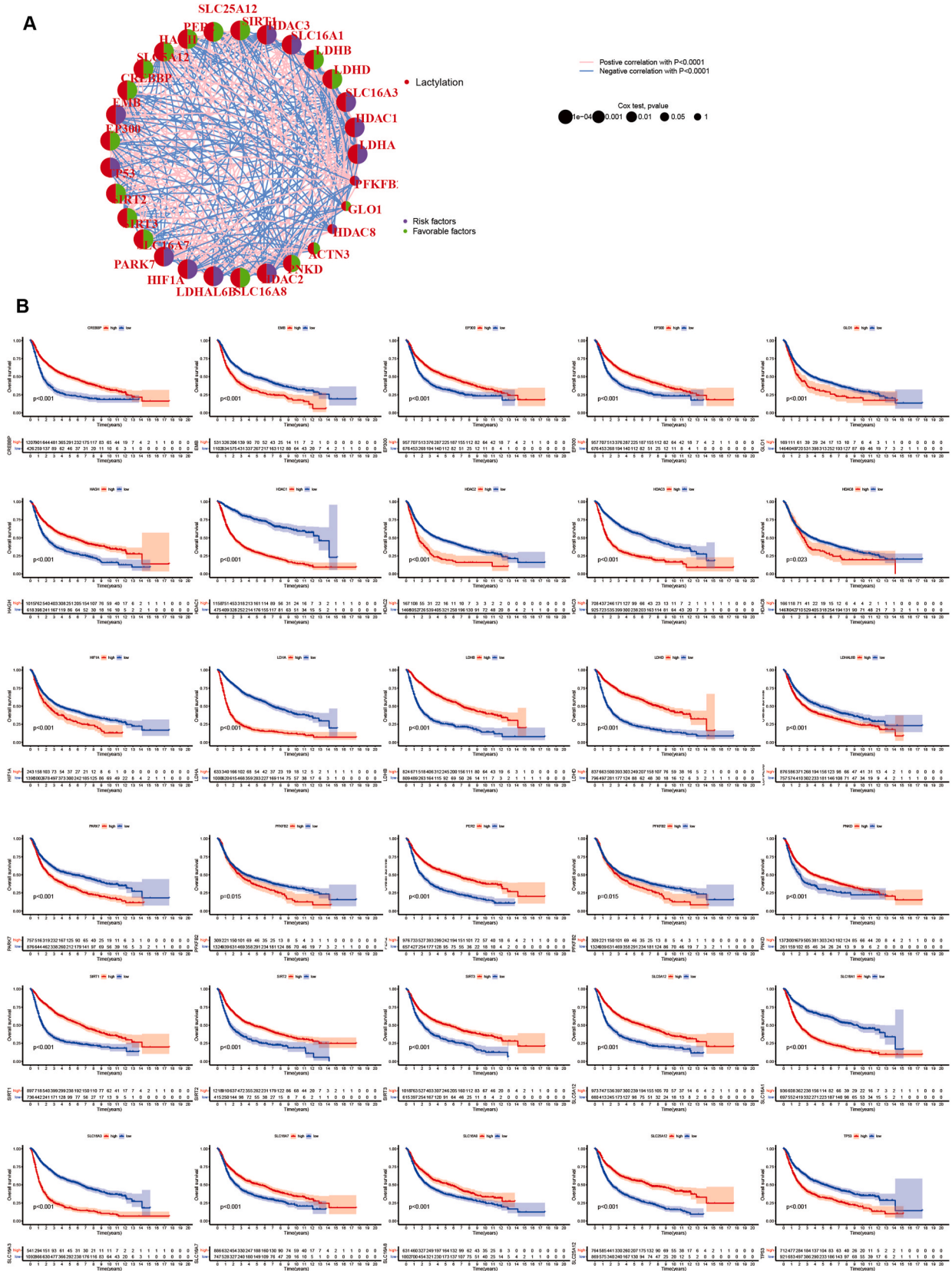


Fig. 4. Lactylation score analysis using the single-cell RNA sequencing data. A. The expression of lactylation-related genes in each cell type. B. The lactylation score values in each cell type. C. The lactylation score and groups are shown using the UAMP plots. D. The percentage of six cell types in the high and low lactylation score groups. E. The scores of 50 hallmark pathways in the high and low lactylation score groups.



(caption on next page)

Fig. 5. Identification of glioma subtypes based on lactylation-related genes

A. Correlation and prognostic values of lactylation-related genes in glioma. The line connecting the lactylation genes represents their correlation, with the line thickness indicating the strength of the correlation among lactylation genes. Blue and pink represent negative and positive correlations, respectively. **B.** Kaplan-Meier analysis of indicated genes. (For interpretation of the references to colour in this figure legend, the reader is referred to the Web version of this article.)

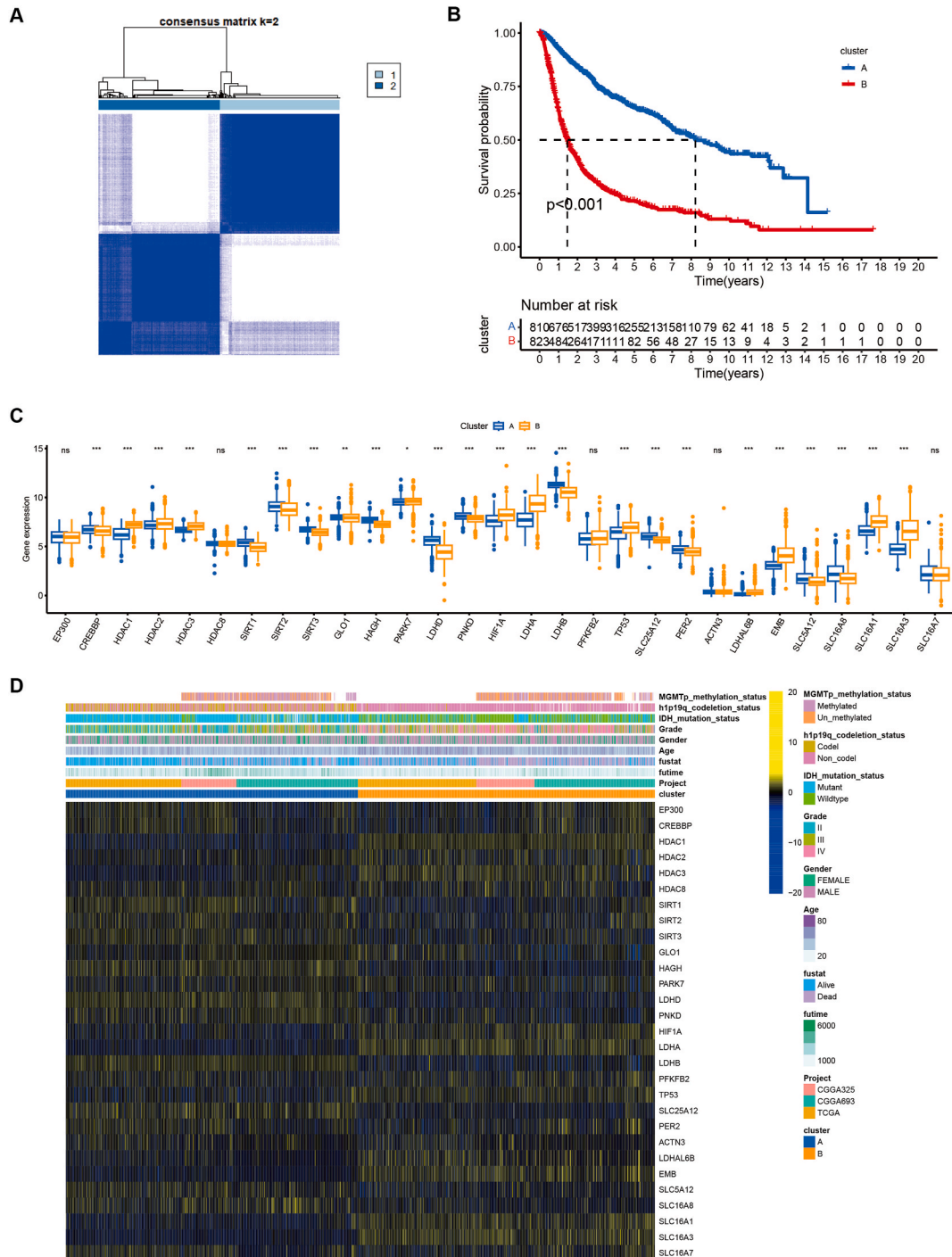
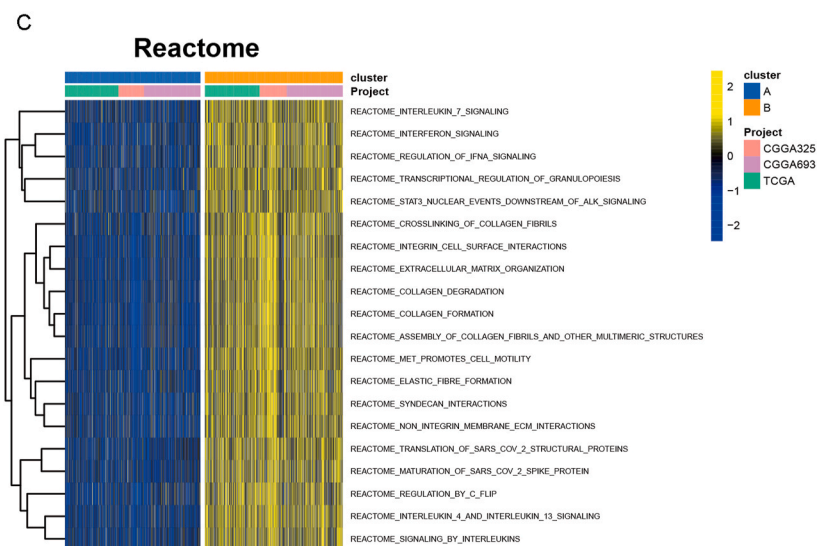
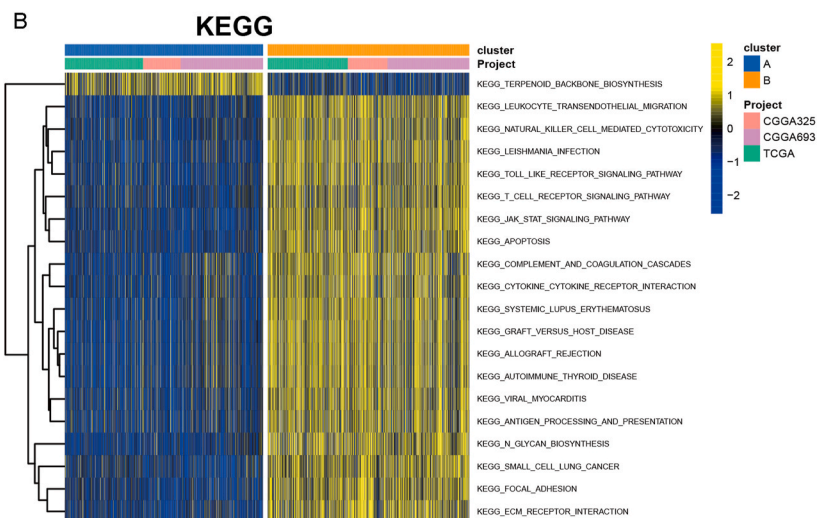
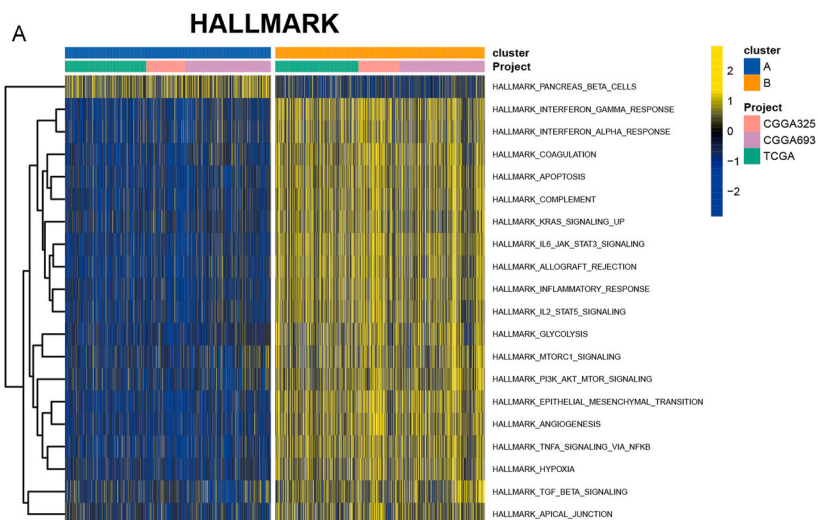


Fig. 6. Identification of subtypes based on lactylation-related genes

A. Consensus matrix heatmap defining various clusters and their correlation area. **B.** Kaplan-Meier analysis of glioma in clusters A and B. **C.** The expression of lactylation-related genes in clusters A and B. **D.** Distributions of clinical features and expression of lactylation-related genes between the two clusters.



(caption on next page)

Fig. 7. The different pathways between the two subtypes
Scores of pathways in two clusters, namely HALLMARK (A), Kyoto Encyclopedia of Genes and Genomes (B) and Reactome pathways (C).

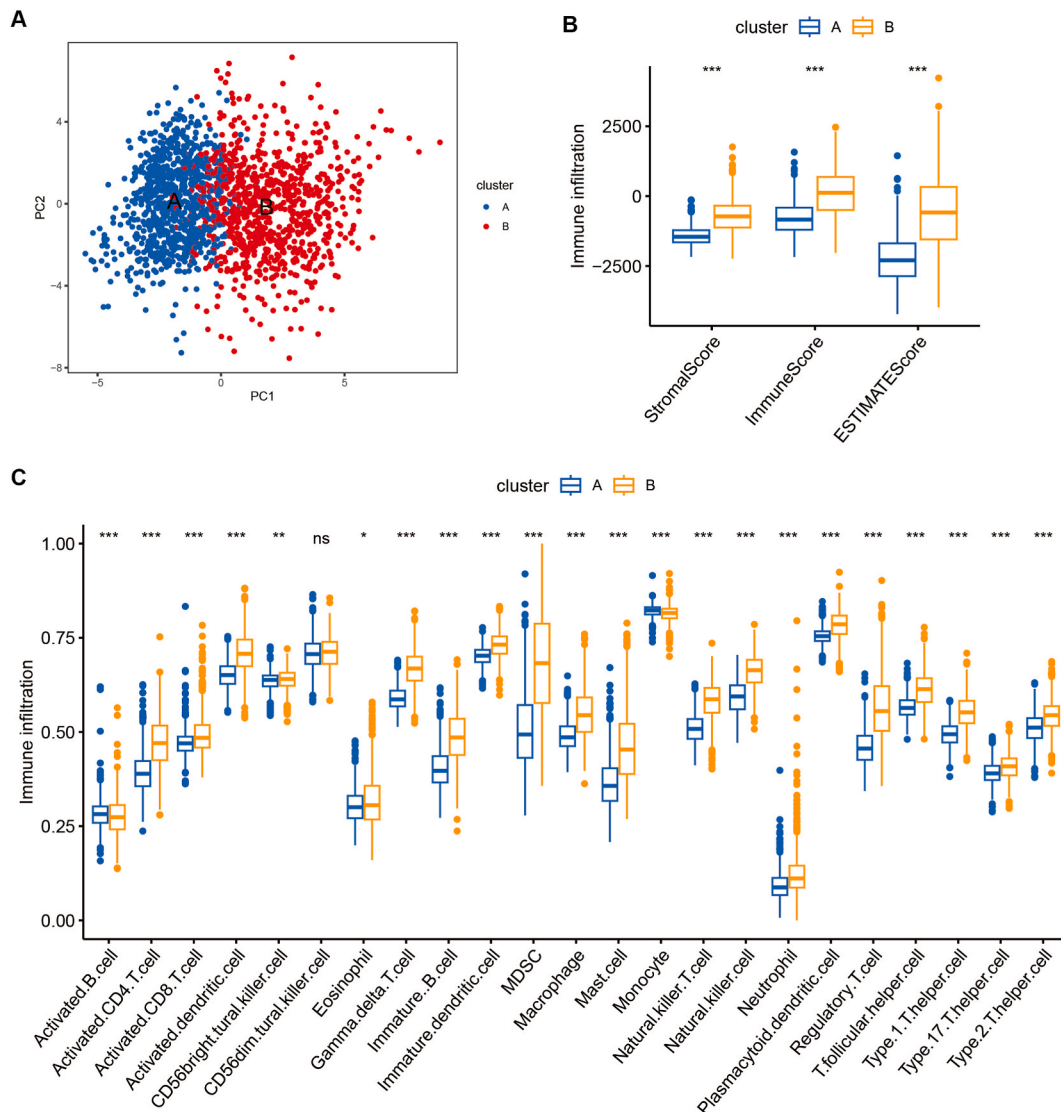


Fig. 8. Immune cell infiltration analysis

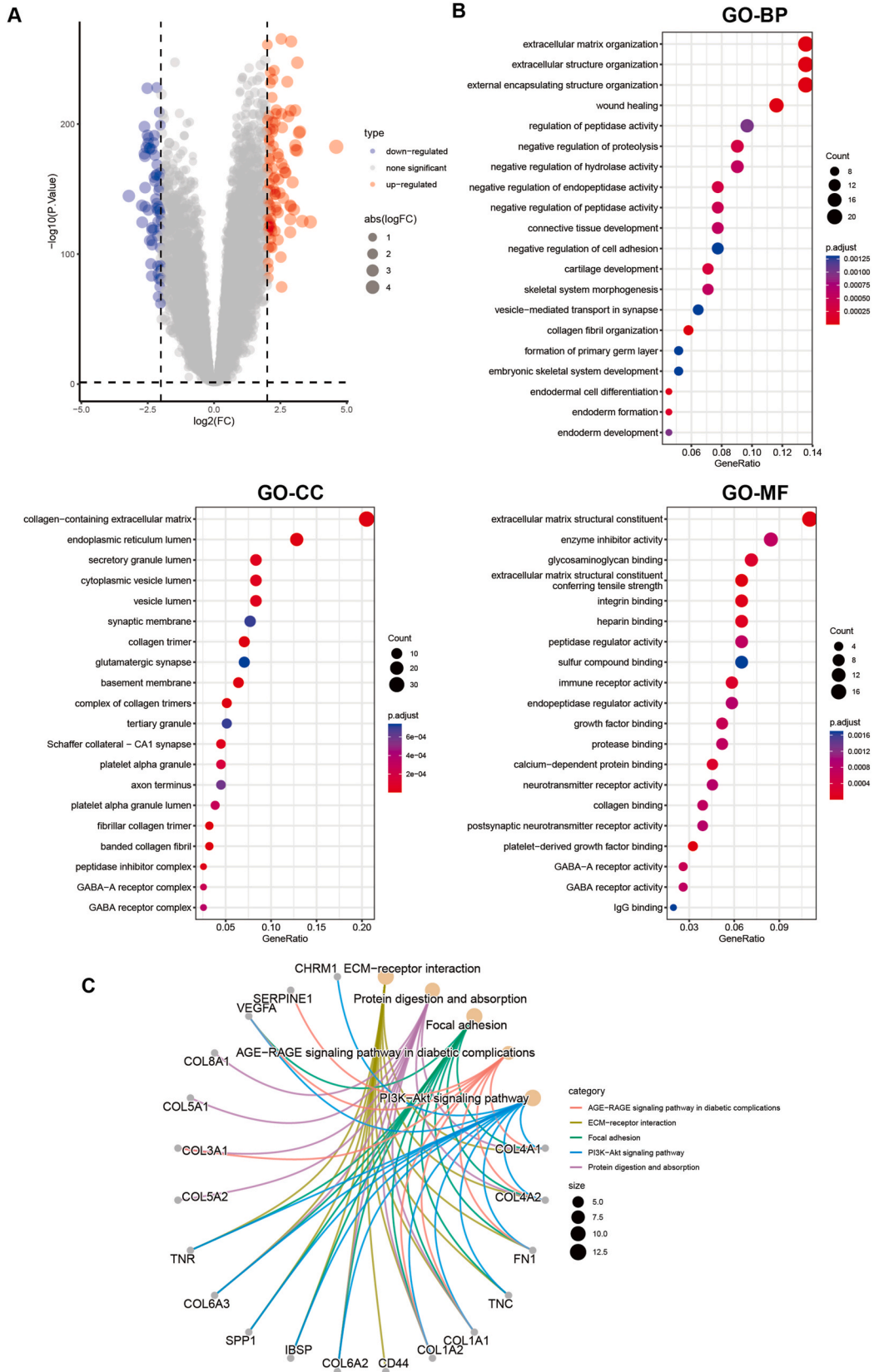
A. Principal component analysis plot of patients with glioma in the two clusters. B. The tumour microenvironment differences in the two clusters. C. The difference in immune cell infiltration level in the two clusters.

demonstrated greater levels of immune cell infiltration than that of cluster A (Fig. 8C).

3.3. Identification of gene subtypes and construction of the lactylation score

In total, 160 DEGs were successfully identified between clusters A and B (Fig. 9A) by utilising the 'limma' package. In the GO enrichment analysis, DEGs were enriched in various biological processes such as extracellular matrix (ECM) organisation, wound healing, negative regulation of proteolysis and collagen fibril organisation. Cellular components were enriched in the collagen-containing ECM and the endoplasmic reticulum lumen. According to molecular function, these were crucial for ECM structural constituents (Fig. 9B). DEGs were predominantly enriched in pathways such as ECM–receptor interaction, protein digestion and absorption, focal adhesion, the advanced glycation end-product (AGE)–receptor for the AGE signalling pathway in diabetic complications and the phosphoinositide 3-kinase–protein kinase B signalling pathway, as evidenced by KEGG analysis (Fig. 9C).

The univariate Cox regression analysis results identified 20 genes that were notably associated with OS to determine the prognostic



(caption on next page)

Fig. 9. Enrichment analysis

A. Volcanic map of differentially expressed genes (DEGs) between the two clusters. B. Gene ontology enrichment analysis of DEGs, including biological progress (BP), cellular component (CC), and molecular function (MF). C. The correlation of DEGs with the top five terms of the Kyoto Encyclopedia of Genes and Genomes results.

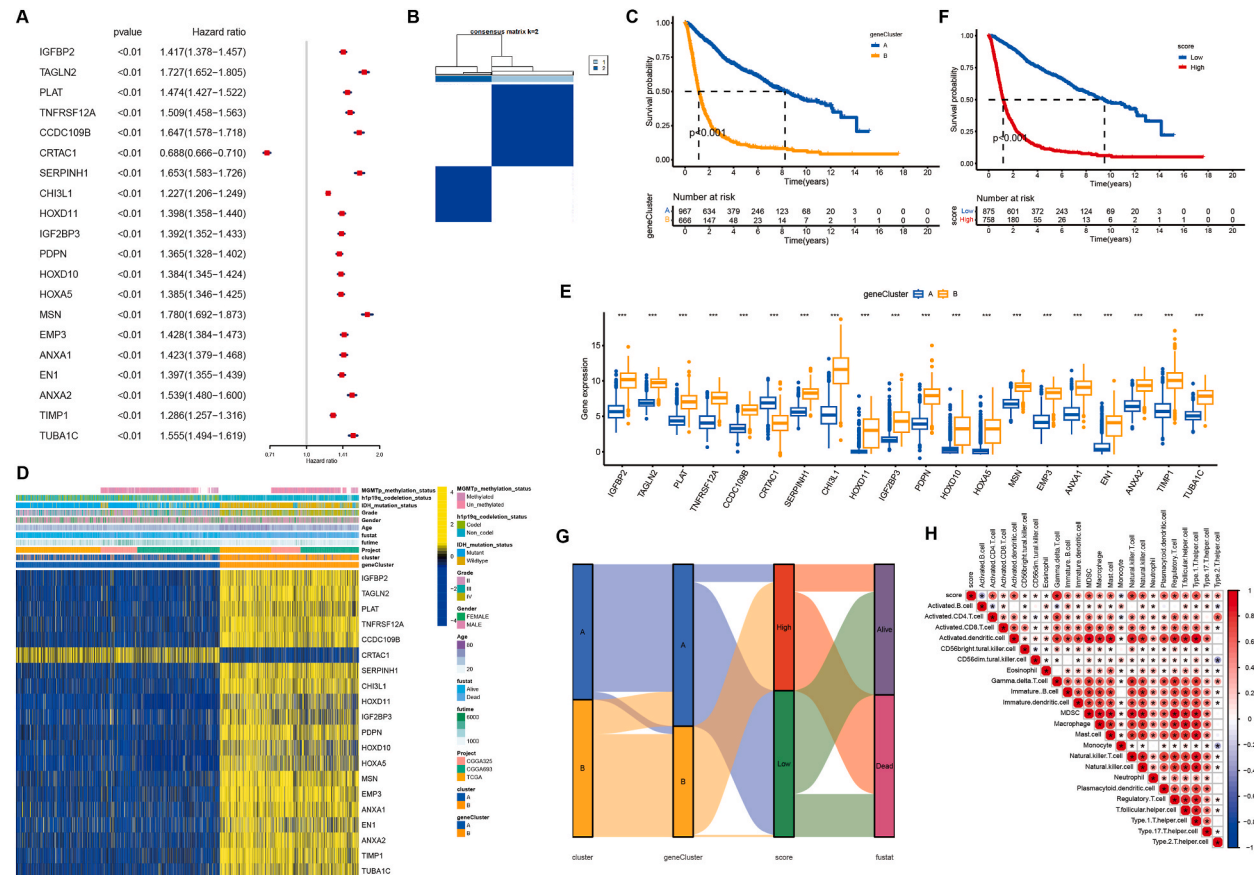


Fig. 10. Construction of lacylation score

A. Forest plot presenting results of univariate Cox regression analysis. B. Consensus matrix heatmap defining various clusters and their correlation area. C. Kaplan–Meier analysis of patients with glioma in the two geneClusters. D. Distributions of clinical features and expression of 20 differentially expressed genes between the two geneClusters. E. The expression of indicated genes in the two geneClusters. F. Kaplan–Meier analysis of lacylation score in glioma. G. The Sankey diagram visualises the correlation between cluster, geneCluster, lacylation score and survival status of patients with glioma. H. The correlation between lacylation score and immune cell infiltration. The red colour represents a positive correlation, and the blue colour represents a negative correlation. (For interpretation of the references to colour in this figure legend, the reader is referred to the Web version of this article.)

significance of the 160 DEGs (Fig. 10A, Supplementary Table 1). Unsupervised clustering results grouped the patients into two subtypes based on the expression of the 20 prognostic genes, hereafter referred to as geneClusters A and B (Fig. 10B). Patients in geneCluster B exhibited worse survival rates than those in geneCluster A (Fig. 10C). The expression of the 20 prognostic genes and the distribution of their clinical features are presented in Fig. 10D and E. The lacylation score, established using PCA with 20 prognostic genes, was used to assess the patient’s prognosis. The patients with high lacylation scores exhibited worse survival outcomes (Fig. 10F). The Sankey diagram represents the correlation between cluster, geneCluster, lacylation score and survival status (Fig. 10G). Analysis of the relationship between the lacylation score and immune cell infiltration revealed that patients with high lacylation scores exhibited increased levels of immune cell infiltration (Fig. 10H).

3.4. Genetic alterations in prognostic genes

We explored the expression and genetic alterations in 20 prognostic genes. Fig. 11A shows the copy number variations (CNVs) for each gene. Homeobox A5 (HOXA5) showed the highest CNV amplification frequency, and cartilage acidic protein 1 (CRTAC1) exhibited a considerable CNV deletion frequency. The percentages of heterozygous and homozygous CNV for each gene in gliomas, including heterozygous and homozygous amplifications and deletions, are shown in Fig. 11B. The linear CNV levels of epithelial

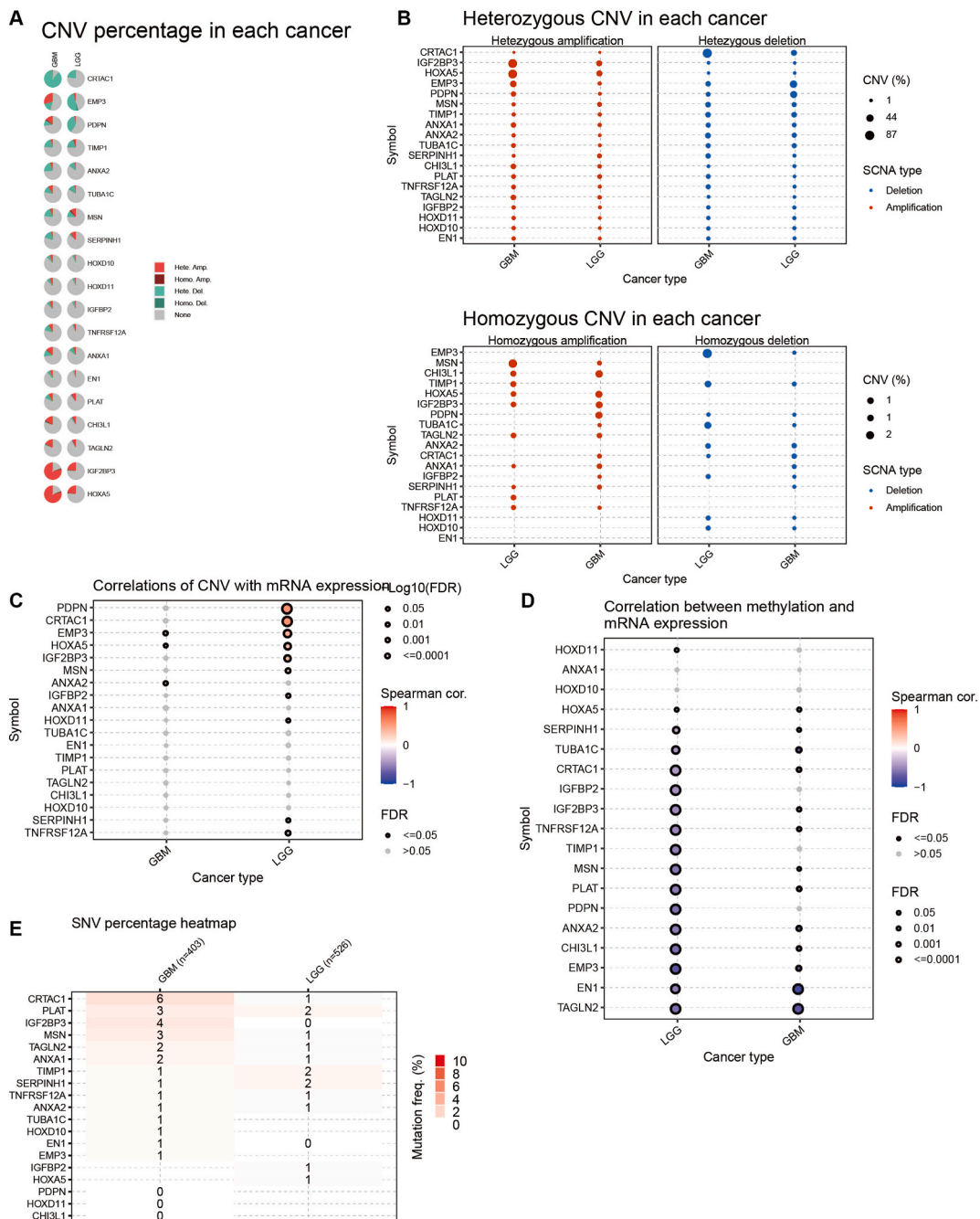


Fig. 11. The genetic alteration of prognostic differentially expressed genes (DEGs) A. The copy-number alteration (CNA) percentage of DEGs in glioma. B. The homozygous and heterozygous copy number variation (CNV) of DEGs in glioma. C. The correlation of CNV with messenger RNA (mRNA) expression in glioma. D. The correlation of methylation level with mRNA expression. E. The frequency of deleterious mutations of lactylation-related genes in glioma.

membrane protein 3 and HOXA5 positively correlated with their corresponding mRNA expression (Fig. 11C). The expression of these genes was negatively correlated with DNA methylation levels (Fig. 11D). The single nucleotide variant (SNV) frequencies of these genes were generally low, with CRTAC1 showing the highest SNV frequency (Fig. 11E).

3.5. Association of lactylation score with clinical features

Live patients presented lower lactylation scores than deceased patients (Fig. 12A). The percentage of patients who survived in the

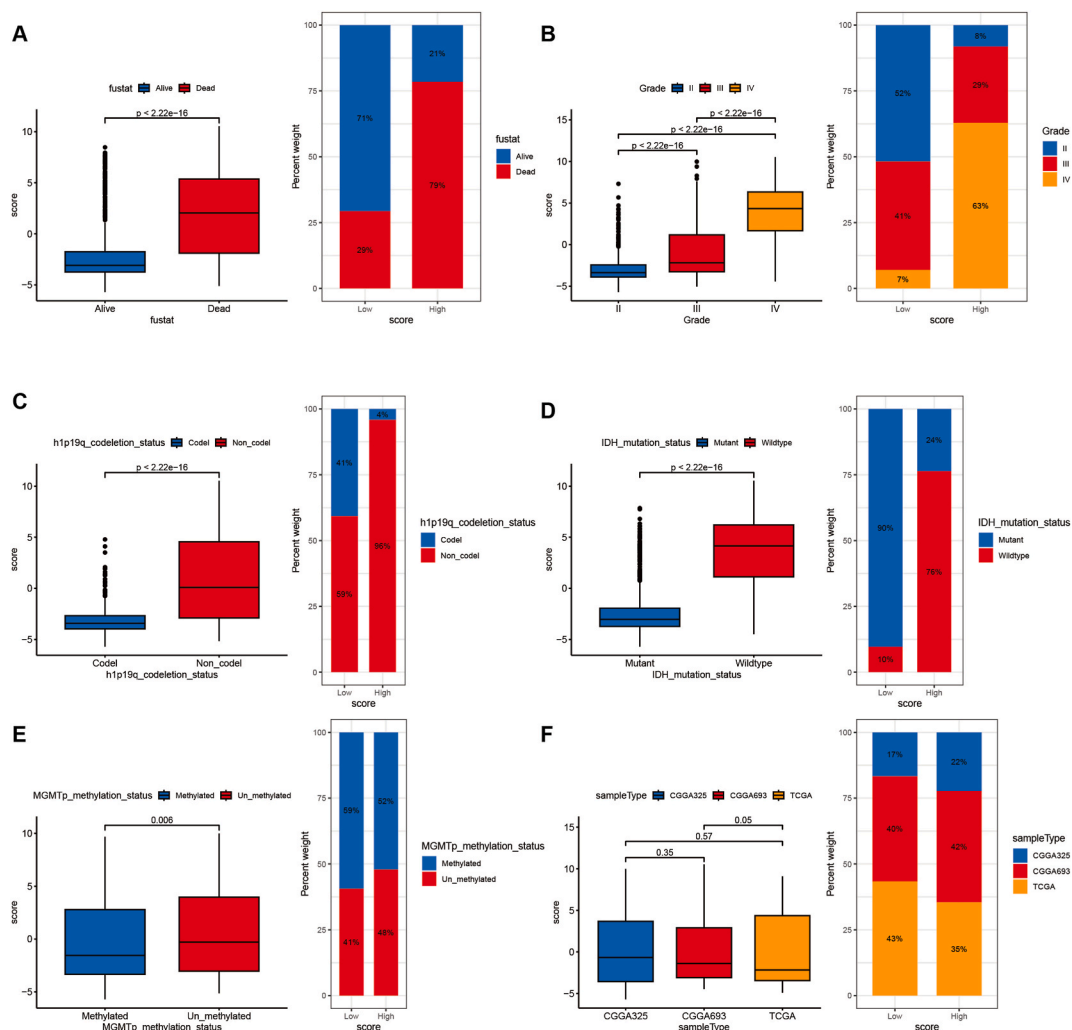


Fig. 12. The association of lactylation scores with clinical features

A. Left: The lactylation score in alive and dead groups. Right: The percentage of alive and dead patients in the high and low lactylation score groups. B. Left: The lactylation score in various grades. Right: The percentage of various grade patients in the high and low lactylation score groups. C. Left: The lactylation score in different h1p19q co-deletion statuses. Right: The percentage of patients with different h1p19q co-deletion status in the high and low lactylation score groups. D. Left: The lactylation score in different isocitrate dehydrogenase (IDH) mutation status. Right: The percentage of patients with different IDH mutation status in the high and low lactylation score groups. E. Left: The lactylation score in different O6-methylguanine-DNA methyltransferase (MGMTp) methylation statuses. Right: The percentage of patients with different MGMTp methylation status in the high and low lactylation score groups. F. Left: The lactylation score in various data sources. Right: The percentage of patients of various data sources in the high and low lactylation score groups.

high lactylation score group (21 %) was lower than that in the low lactylation score group (71 %). Moreover, a higher lactylation score was significantly linked to other malignant clinical characteristics, such as a higher tumour grade (Fig. 12B), non-co-deletion of h1p19q (Fig. 12C), wild-type isocitrate dehydrogenase (Fig. 12D) and O6-methylguanine-DNA methyltransferase unmethylation (Fig. 12E). There were no significant differences in lactylation scores among patients with glioma from different data sources (Fig. 12F).

3.6. Correlation of lactylation score with immune microenvironment and immunotherapeutic efficacy

The correlation between the immune microenvironment and the lactylation score was evaluated. Chemokine and receptor expression were notably increased in the high lactylation score category (Fig. 13A). The lactylation score correlated favourably with immune-related pathways, such as INTERFERON GAMMA RESPONSE and INFLAMMATORY RESPONSE (Fig. 13B).

The high lactylation score group presented increased expression of the immune checkpoints CD274, cytotoxic T-lymphocyte associated protein 4, lymphocyte activation gene 3 and programmed cell death protein 1 (Supplemental Fig. 1). Moreover, the high

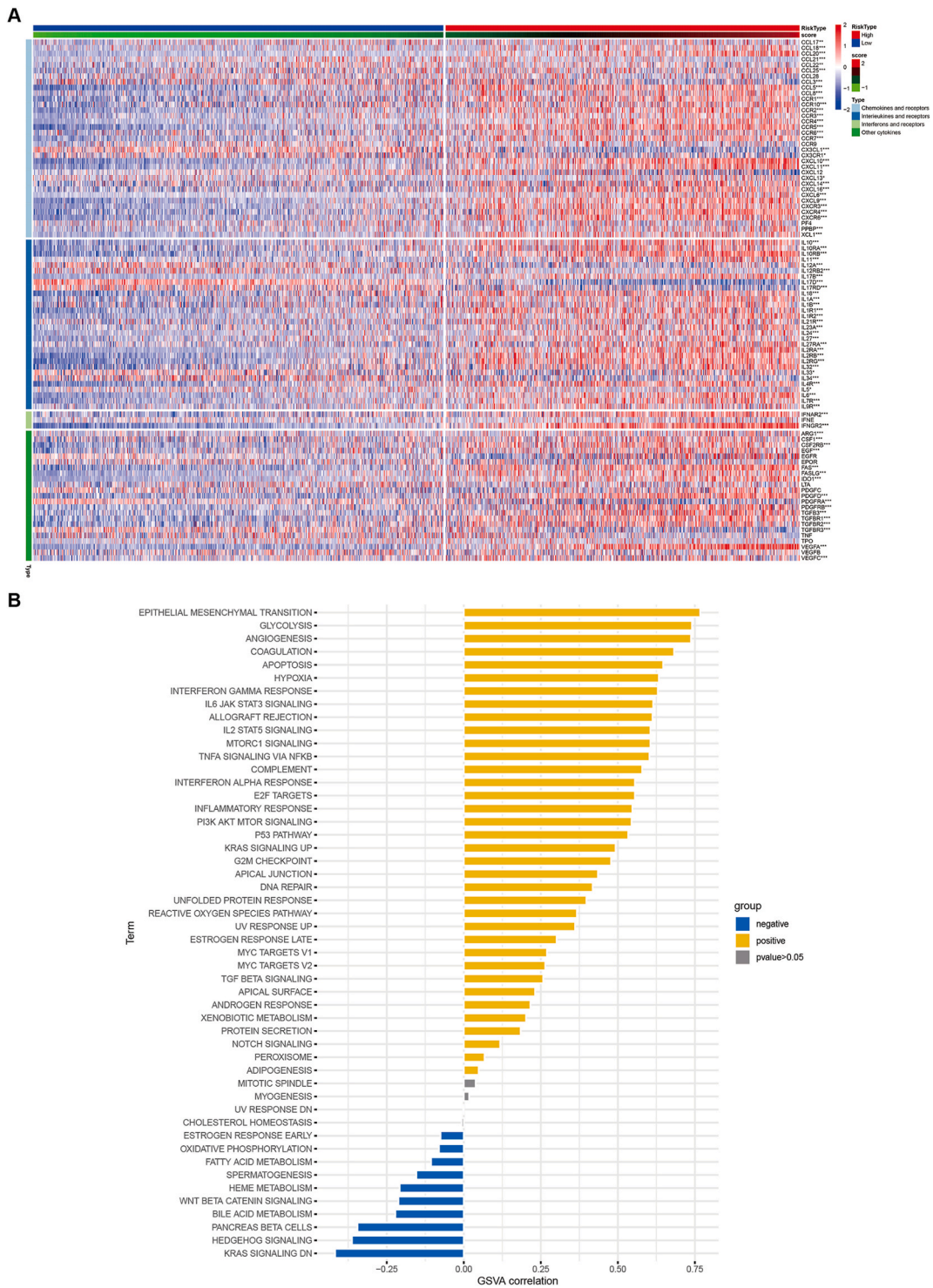


Fig. 13. The association of lactylation score with immune-related genes
 A. The expression of chemokines and chemokine receptors in the high and low lactylation score groups in glioma. B. The correlation of lactylation score with HALLMARK pathway scores.

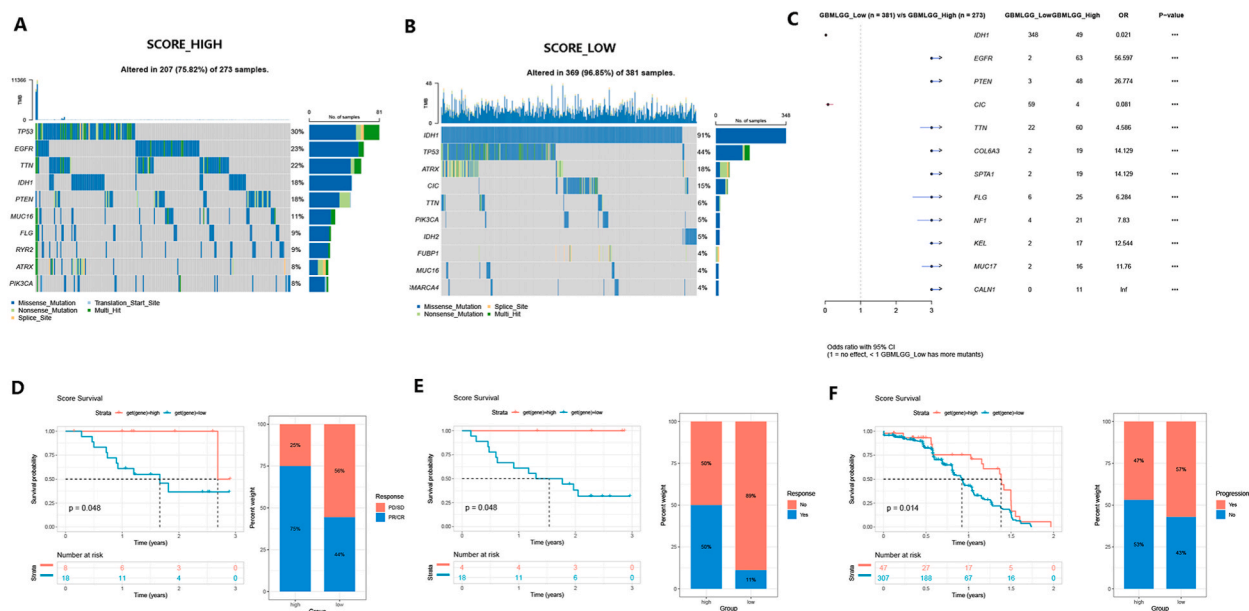


Fig. 14. Gene mutations and the role of lactylation score in predicting the efficiency of immune checkpoint inhibitor (ICI) treatment
A-B. Distribution of top 12 mutated genes in the high- and low-score groups. C. Comparison of the gene mutations in the high and low lactylation score groups. D. Left: Kaplan–Meier analysis of patients in high and low lactylation score groups in the GSE78220 cohort. Right: The percentage of patients with different progress statuses after ICI treatment in the high and low lactylation score groups in the GSE78220 cohort. E. Left: Kaplan–Meier analysis of patients in the high and low lactylation score groups in the Riaz2017 cohort. Right: The percentage of patients with different progress statuses after ICI treatment in the high and low lactylation score groups in the Riaz2017 cohort. F. Left: Kaplan–Meier analysis of patients in the high and low lactylation score groups in the NCT02684006 cohort. Right: The percentage of patients with different progress statuses after ICI treatment in the high and low lactylation score groups in the NCT02684006 cohort.

lactylation score group presented a higher frequency of gene mutations (Fig. 14A–C). Additionally, a higher level of cell–cell communication was observed in the high lactylation score, according to scRNA analysis (Supplementary Fig. 2). These findings further support the theory that patients with cancer with high lactylation scores respond well to immunotherapy.

Further analyses were performed using immunotherapy datasets to verify our hypotheses. We confirmed that patients with high lactylation scores were responsive to immune checkpoint inhibitor (ICI) treatment in the GSE78220 dataset (Fig. 14D; melanoma), Riaz2017 cohort (Fig. 14E; melanoma), and NCT02684006 cohort (Fig. 14F; Renal clear cell carcinoma). In addition to analysing immunotherapeutic responses, traditional anti-tumour medications were examined. Utilising the R package ‘pRRophetic,’ six anti-tumour drugs that could potentially be ineffective for patients with a high lactylation score and six anti-tumour drugs that may be beneficial for patients with a high lactylation score were identified (Fig. 15).

4. Discussion

Lactylation modification is a promising field of research in cancer therapeutics. Tumour cells undergo metabolic reprogramming, resulting in increased lactate production and alterations in their microenvironment [14,15]. Lactate is crucial for tumour growth and progression because it enhances angiogenesis, immune evasion and metastasis [16]. Protein lactylation modulates carcinogenesis-associated cellular processes, including survival, proliferation and invasion [17,18]. These findings suggest that lactylation may be a novel therapeutic target for cancer treatment. Further studies are needed to identify specific lactylation-related targets and investigate the underlying mechanisms in different tumour types.

In recent years, lactylation modifications in cancer have garnered increasing attention. Various studies have investigated the role of lactylation in specific tumour types such as lung [19], liver [18,20] and gastric [21] cancers. Overall, emerging evidence suggests that lactylation is important in cancer pathogenesis and progression. Further studies are needed to explore the underlying mechanisms of lactylation in different tumour types and develop novel lactylation-based therapies for cancer treatment.

Herein, we evaluated lactylation-related genes and lactylation scores in gliomas using scRNA-seq data. We identified the following six core cell types: mono, macro, microglia, endothelial cells, DC, fibroblasts and CD8 T cells. Additionally, we calculated the lactylation score and 50 hallmark pathways using the RNA-seq data. The lactylation process was found to be closely associated with ADIPOGENESIS, DNA REPAIR, MTORC1 SIGNALING and OXIDATIVE PHOSPHORYLATION pathways in all cell types. The lactylation score was the highest in microglial cells and the lowest in fibroblast cells. The percentage of microglial cells was higher in the high lactylation score group than in the low lactylation score group. These results indicate that microglial cells undergo lactylation most frequently in gliomas. Lactylation of Yin Yang 1 in microglia promotes angiogenesis through transcriptional activation-mediated up-

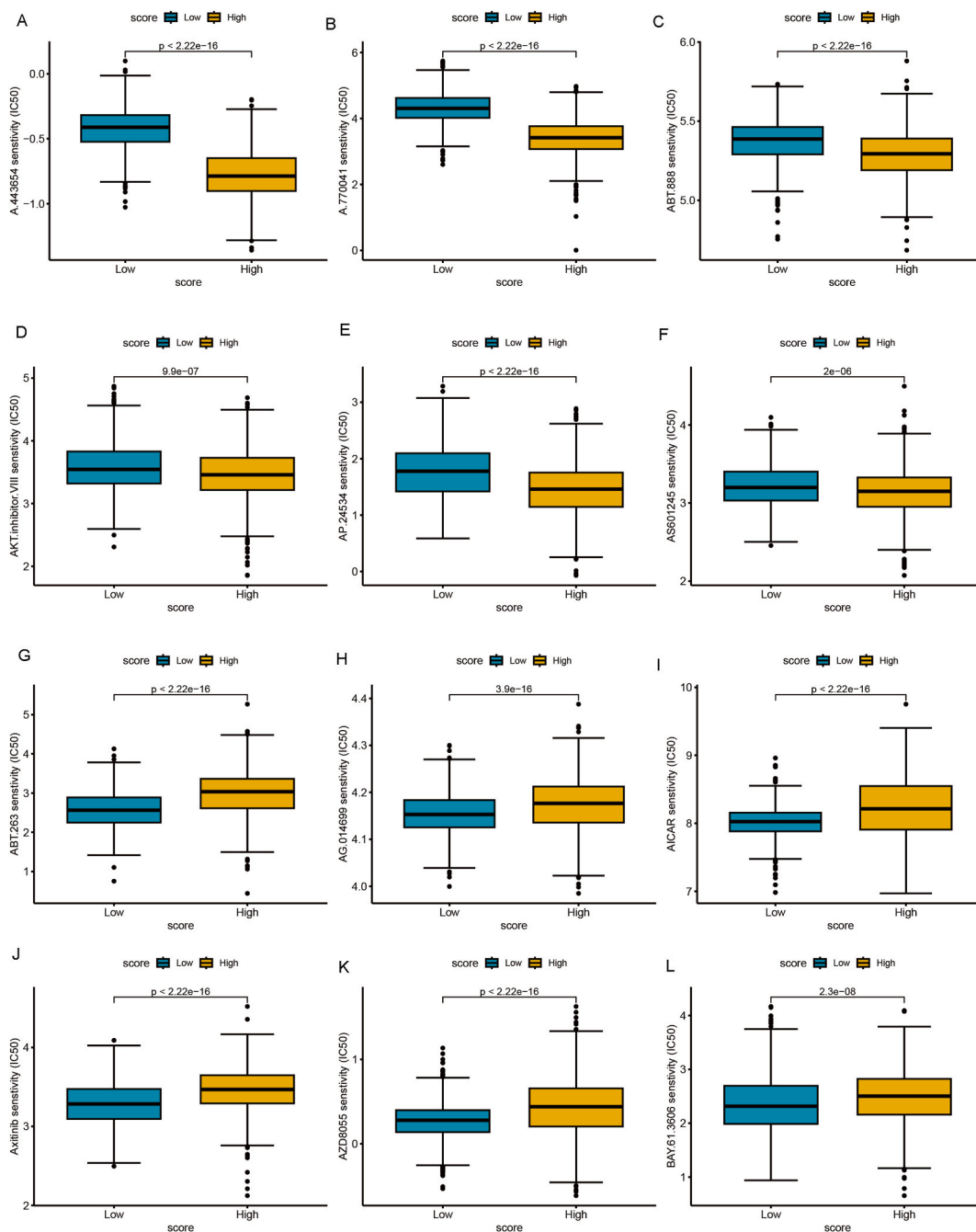


Fig. 15. The analysis of curative effect of anti-tumour drugs

The 50 % maximum inhibitory concentration values of the indicated antitumour drugs in the high and low lactylation score groups. A: A.443654 sensitivity. B: A.770041 sensitivity. C: ABT.888 sensitivity. D: AKT.inhibitor.VIII sensitivity. E: AP.24534 sensitivity. F: AS601245 sensitivity. G: ABT.263 sensitivity. H: AG.014699 sensitivity. I: AICAR sensitivity. J: Axitinib sensitivity. K: AZD8055 sensitivity. L: BAY.61.3606 sensitivity.

regulation of fibroblast growth factor 2 [22], consistent with our results. Therefore, lactylation modifications in microglial cells must be explored.

By examining the expression of lactylation-related genes, we identified two glioma subtypes (clusters A and B). Differences were observed between the malignant cancer-promoting and immune-related pathways between clusters A and B, including TGF BETA SIGNALING. Therefore, we assessed immune infiltration in glioma samples. The stromal, immune, and ESTIMATE scores were higher in cluster B, and most immune cells showed higher infiltration in cluster B than those in cluster A.

A lactylation scoring that could effectively measure risk in patients was constructed. In total, 160 DEGs were examined between the

two groups. Using univariate Cox regression analysis, the predictive significance of these 160 DEGs was evaluated and 20 genes that were strongly associated with OS were identified. Using PCA, a lactylation scoring for these 20 genes was developed. Patients with higher lactylation scores exhibited lower survival rates. The association between lactylation scores and immune cell infiltration indicated a positive association between these two factors.

The effectiveness of ICI treatment can be predicted by chemokines, chemokine receptors and immune checkpoints [23,24]. The high lactylation score group showed higher expression of chemokines, chemokine receptors and immune checkpoints, indicating that these patients may respond better to ICI treatment. Additionally, we observed high immune cell infiltration and cell–cell communication in the high-score group. High immune infiltration and cellular communication levels often indicate the activity of immune cells in the tumour microenvironment [25,26]. Therefore, we speculate that patients with high scores may be more sensitive to immunotherapy. The analysis of the immunotherapy datasets confirmed that patients with high lactylation scores responded positively to ICI treatment in the GSE78220, Riaz2017 and NCT02684006 cohorts.

Our study has some limitations. First, owing to data limitations, immunotherapy data for large sample sizes of gliomas are lacking. Next, further experimental exploration is required for key genes in the lactylation scores.

In conclusion, our comprehensive analysis of lactylation-related genes revealed their substantial effects on the immune micro-environment and outcomes of patients with glioma. The developed lactylation scoring showed its efficacy in predicting the prognosis and response to ICI therapy. These results underscore the critical importance of lactylation in clinical decision-making, providing a novel approach for the personalised treatment of patients with glioma.

Funding

This work was supported by grants from the Innovation Project of Clinical Science and Technology of Jinan City [grant nos. 202225040 and 202134057], Preferential Subsidy Research Project to Postdoctoral of Jiangxi Province [grant no.2021KY39], Scientific and Technological Research Project of Shandong Geriatrics Society [grant no. LEJGG2021W058] and the Taishan Scholar Program of Shandong Province [grant no. tstp20230659].

Data availability statement

All the data analysis results obtained during this study are included in the manuscript and its Supplementary Information. The original contributions presented in this study can be obtained upon request by contacting the corresponding author via email.

CRediT authorship contribution statement

Xiangdong Lu: Writing – review & editing, Writing – original draft, Funding acquisition. **Zijian Zhou:** Writing – review & editing, Formal analysis, Data curation. **Peng Qiu:** Writing – review & editing, Conceptualization. **Tao Xin:** Writing – review & editing, Funding acquisition, Conceptualization.

Declaration of competing interest

The authors declare that they have no known competing financial interests or personal relationships that could have appeared to influence the work reported in this paper.

Acknowledgements

Not applicable.

Appendix A. Supplementary data

Supplementary data to this article can be found online at <https://doi.org/10.1016/j.heliyon.2024.e30726>.

References

- [1] S. Xu, L. Tang, X. Li, F. Fan, Z. Liu, Immunotherapy for glioma: Current management and future application, *Cancer Lett.* 476 (2020) 1–12.
- [2] F. Yasinjan, Y. Xing, H. Geng, R. Guo, L. Yang, Z. Liu, et al., Immunotherapy: a promising approach for glioma treatment, *Front. Immunol.* 14 (2023) 1255611.
- [3] D. Zhang, Z. Tang, H. Huang, G. Zhou, C. Cui, Y. Weng, et al., Metabolic regulation of gene expression by histone lactylation, *Nature* 574 (7779) (2019) 575–580.
- [4] J. Yu, P. Chai, M. Xie, S. Ge, J. Ruan, X. Fan, et al., Histone lactylation drives oncogenesis by facilitating m(6)A reader protein YTHDF2 expression in ocular melanoma, *Genome Biol.* 22 (1) (2021) 85.
- [5] K. Yang, M. Fan, X. Wang, J. Xu, Y. Wang, F. Tu, et al., Lactate promotes macrophage HMGB1 lactylation, acetylation, and exosomal release in polymicrobial sepsis, *Cell Death Differ.* 29 (1) (2022) 133–146.
- [6] N. Wang, W. Wang, X. Wang, G. Mang, J. Chen, X. Yan, et al., Histone lactylation boosts Reparative gene activation post-Myocardial infarction, *Circ. Res.* 131 (11) (2022) 893–908.

- [7] F.A. Peccatori, B. Migliavacca Zucchetti, B. Buonomo, G. Bellettini, G. Codacci-Pisanelli, M. Notarangelo, Lactation during and after breast cancer, *Adv. Exp. Med. Biol.* 1252 (2020) 159–163.
- [8] Z. Miao, X. Zhao, X. Liu, Hypoxia induced β -catenin lactylation promotes the cell proliferation and stemness of colorectal cancer through the wnt signaling pathway, *Exp. Cell Res.* 422 (1) (2023) 113439.
- [9] L. Pan, F. Feng, J. Wu, S. Fan, J. Han, S. Wang, et al., Demethylzylalateral targets lactate by inhibiting histone lactylation to suppress the tumorigenicity of liver cancer stem cells, *Pharmacol. Res.* 181 (2022) 106270.
- [10] L. Li, Z. Li, X. Meng, X. Wang, D. Song, Y. Liu, et al., Histone lactylation-derived LINC01127 promotes the self-renewal of glioblastoma stem cells via the cis-regulating the MAP4K4 to activate JNK pathway, *Cancer Lett.* 579 (2023) 216467.
- [11] T. Sun, B. Liu, Y. Li, J. Wu, Y. Cao, S. Yang, et al., Oxamate enhances the efficacy of CAR-T therapy against glioblastoma via suppressing ectonucleotidases and CCR8 lactylation, *J. Exp. Clin. Cancer Res.* : CR 42 (1) (2023) 253.
- [12] X. Liu, Y. Zhang, W. Li, X. Zhou, Lactylation, an emerging hallmark of metabolic reprogramming: current progress and open challenges, *Front. Cell Dev. Biol.* 10 (2022) 972020.
- [13] Z. Yang, X. Ming, S. Huang, M. Yang, X. Zhou, J. Fang, Comprehensive analysis of m(6)A regulators characterized by the immune cell infiltration in head and neck squamous cell carcinoma to aid immunotherapy and chemotherapy, *Front. Oncol.* 11 (2021) 764798.
- [14] R. Sgarra, S. Battista, L. Cerchia, G. Manfioletti, M. Fedele, Mechanism of action of lactic acid on histones in cancer, *Antioxidants Redox Signal.* (2023).
- [15] Y. Xu, X. Hao, Y. Ren, Q. Xu, X. Liu, S. Song, et al., Research progress of abnormal lactate metabolism and lactate modification in immunotherapy of hepatocellular carcinoma, *Front. Oncol.* 12 (2022) 1063423.
- [16] L. Wang, S. Li, H. Luo, Q. Lu, S. Yu, PCSK9 promotes the progression and metastasis of colon cancer cells through regulation of EMT and PI3K/AKT signaling in tumor cells and phenotypic polarization of macrophages, *J. Exp. Clin. Cancer Res.* : CR 41 (1) (2022) 303.
- [17] X. Wang, T. Ying, J. Yuan, Y. Wang, X. Su, S. Chen, et al., BRAFV600E restructures cellular lactylation to promote anaplastic thyroid cancer proliferation, *Endocr. Relat. Cancer* 30 (8) (2023).
- [18] X. Wu, In-depth discovery of protein lactylation in hepatocellular carcinoma, *Proteomics* 23 (9) (2023) e2300003.
- [19] Y.H. Yang, Q.C. Wang, J. Kong, J.T. Yang, J.F. Liu, Global profiling of lysine lactylation in human lungs, *Proteomics* (2023) e2200437.
- [20] E. Kotsiliti, Lactylation and HCC progression, *Nat. Rev. Gastroenterol. Hepatol.* 20 (3) (2023) 131.
- [21] H. Yang, X. Zou, S. Yang, A. Zhang, N. Li, Z. Ma, Identification of lactylation related model to predict prognostic, tumor infiltrating immunocytes and response of immunotherapy in gastric cancer, *Front. Immunol.* 14 (2023) 1149989.
- [22] X. Wang, W. Fan, N. Li, Y. Ma, M. Yao, G. Wang, et al., YY1 lactylation in microglia promotes angiogenesis through transcription activation-mediated upregulation of FGF2, *Genome Biol.* 24 (1) (2023) 87.
- [23] D.J. Pinato, S. Howlett, D. Ottaviani, H. Urus, A. Patel, T. Mineo, et al., Association of prior antibiotic treatment with survival and response to immune checkpoint inhibitor therapy in patients with cancer, *JAMA Oncol.* 5 (12) (2019) 1774–1778.
- [24] L. Liu, X. Bai, J. Wang, X.R. Tang, D.H. Wu, S.S. Du, et al., Combination of TMB and CNA stratifies prognostic and predictive responses to immunotherapy across metastatic cancer, *Clin. Cancer Res. : an official journal of the American Association for Cancer Research* 25 (24) (2019) 7413–7423.
- [25] K. Bridges, K. Miller-Jensen, Mapping and validation of scRNA-seq-derived cell-cell communication networks in the tumor microenvironment, *Front. Immunol.* 13 (2022) 885267.
- [26] L.X. Chen, S.J. Zeng, X.D. Liu, H.B. Tang, J.W. Wang, Q. Jiang, Cell-cell communications shape tumor microenvironment and predict clinical outcomes in clear cell renal carcinoma, *J. Transl. Med.* 21 (1) (2023) 113.